Protein Science (1999), *8*:298–306. Cambridge University Press. Printed in the USA.

Crystal structure of the FMN-binding domain of human cytochrome P450 reductase at 1.93 Å resolution

QIANG ZHAO,[1] SANDEEP MODI,[3] GRAEME SMITH,[2] MARK PAINE,[2]
PAUL D. McDONAGH,[3] C. ROLAND WOLF,[2] DAVID TEW,[4] LU-YUN LIAN,[3]
GORDON C.K. ROBERTS,[3] AND HUUB P.C. DRIESSEN[1]

[1]ICRF Unit of Structural Molecular Biology, Department of Crystallography, Birkbeck College, London WC1E 7HX, United Kingdom
[2]ICRF Molecular Pharmacology Unit, University of Dundee, Biomedical Research Centre, Ninewells Hospital and Medical School, University of Dundee, Dundee DDl 9SY, United Kingdom
[3]Centre for Mechanisms of Human Toxicity, Department of Biochemistry and Biological NMR Centre, University of Leicester, P.O. Box 138, Lancaster Road, Leicester LEl 9HN, United Kingdom
[4]Smith Kline Beecham Research, The Frythe, Welwyn, Hertfordshire AR6 9AR, United Kingdom

(RECEIVED August 5, 1998; ACCEPTED November 3, 1998)

Abstract

The crystal structure of the FMN-binding domain of human NADPH-cytochrome P450 reductase (P450R-FMN), a key component in the cytochrome P450 monooxygenase system, has been determined to 1.93 Å resolution and shown to be very similar both to the global fold in solution (Barsukov I et al., 1997, *J Biomol NMR 10*:63–75) and to the corresponding domain in the 2.6 Å crystal structure of intact rat P450R (Wang M et al., 1997, *Proc Nat Acad Sci USA 94*:8411–8416). The crystal structure of P450R-FMN reported here confirms the overall similarity of its α-β-α architecture to that of the bacterial flavodoxins, but reveals differences in the position, number, and length of the helices relative to the central β-sheet. The marked similarity between P450R-FMN and flavodoxins in the interactions between the FMN and the protein, indicate a striking evolutionary conservation of the FMN binding site. The P450R-FMN molecule has an unusual surface charge distribution, leading to a very strong dipole, which may be involved in docking cytochrome P450 into place for electron transfer near the FMN. Several acidic residues near the FMN are identified by mutagenesis experiments to be important for electron transfer to P450 2D6 and to cytochrome *c*, a clear indication of the part of the molecular surface that is likely to be involved in substrate binding. Somewhat different parts are found to be involved in binding cytochrome P450 and cytochrome *c*.

Keywords: domains; flavoprotein; P450; P450 reductase; structure

NADPH-cytochrome P450 oxidoreductase (P450R) is an essential component of the cytochrome P450 monooxygenase system found in the endoplasmic reticulum of eukaryotic cells (Philips & Langdon, 1962; Williams & Kamin, 1962; Lu et al., 1969), which plays a crucial role in the metabolism of drugs and xenobiotics (Ortiz de Montellano, 1995). P450R is a 78 kDa membrane-bound flavoprotein, containing one molecule each of FMN and FAD (Iyanagi & Mason, 1973), which transfers electrons from NADPH to the cytochromes P450. The enzyme can also transfer electrons to cytochrome b_5 (Enoch & Strittmatter, 1979), haem oxygenase (Schacter et al., 1972), and the fatty acid elongation system (Ilan et al., 1981) and to exogenous electron acceptors including cytochrome *c* (Williams & Kamin, 1962).

Reprint requests to: Huub Driessen, ICRF Unit of Structural Molecular Biology, Department of Crystallography, Birkbeck College, London WC1E 7HX, United Kingdom; e-mail: h.driessen@mail.cryst.bbk.ac.uk.

Cytochrome P450 reductase is a multidomain protein, comprising three separable domains: a hydrophobic N-terminal domain, which anchors the enzyme to the membrane, an FMN-binding domain, and an FAD/NADPH-binding domain (Porter, 1991; Porter & Kasper, 1986; Smith et al., 1994). The FAD/NADPH binding domain shows clear sequence homology to ferredoxin-$NADP^+$ reductase and NADH-cytochrome b_5 reductase (Porter & Kasper, 1986; Karplus et al., 1991) and the FMN-binding domain to several bacterial FMN-containing flavodoxins (Porter & Kasper, 1986). The FAD moiety serves as the initial acceptor of electrons from NADPH, transferring them to the FMN and thence to the haem iron of cytochrome P450.

As yet, only limited structural information is available for the components of the microsomal mono-oxygenase system. No structure has yet been determined for any mammalian P450, although models have been constructed (e.g., Modi et al., 1996). The medium-resolution (2.6 Å) three-dimensional crystal structure of an

N-terminally truncated P450 reductase from rat liver was described (Wang et al., 1997) while the present paper was being prepared for publication.

The FMN-binding and NADPH/FAD-binding domains of human P450 reductase have been individually expressed (Smith et al., 1994; Barsukov et al., 1997) and crystallized (Zhao et al., 1996) and the global fold of the FMN-binding domain has been determined by NMR (Barsukov et al., 1997). The purified FMN and FAD/NADPH domains can be reconstituted to form a complex, which has significant catalytic activity in the reduction of cytochrome *c* and in donating electrons for cytochrome P450-dependent monooxygenase reactions (Smith et al., 1994; Barsukov et al., 1997). We now describe the high-resolution structure of the FMN-binding domain of human P450 reductase (P450R-FMN) as determined by X-ray crystallography. We compare the structure of P450R-FMN with the known structures of homologous flavodoxins and intact rat P450R (Wang et al., 1997). The FMN-binding domain of P450R is of particular importance as the part of the enzyme that interacts with cytochromes P450, both to transfer electrons and in some cases to influence substrate binding to the P450 (Modi et al., 1997). Residues that may be involved in this interaction are discussed on the basis of the structures of P450R-FMN, the intact rat reductase (Wang et al., 1997) and the haemoprotein domain of *Bacillus megaterium* P450 BM-3 (Ravichandran et al., 1993), and the results of site-directed mutagenesis experiments.

Materials and methods

Cloning, protein purification, and crystallization

The functional FMN binding domain of human fibroblast P450 reductase was expressed and crystallized as described previously (Smith et al., 1994; Zhao et al., 1996; Barsukov et al., 1997). Electrospray mass spectrometry (measured M_r 20,225 Da) indicated that the crystals contained a protein consisting of the four residues GSHM introduced by the expression system, followed by residues Thr61 to Ser245, representing exons 3–7 of P450R. In this paper Thr61 of the intact reductase is residue 1.

Derivatives and data collection

Heavy atom derivatives were prepared by soaking the crystals in mother liquor with heavy atom compounds in the dark. Data were collected on 30 and 18 cm diameter MAR image plates mounted on Siemens XP-18 and GEC-Elliott GX-21 X-ray generators, respectively (graphite monochromated CuKα). Each data set was collected from a single crystal at a temperature of 14 °C. All X-ray data sets were processed with the program DENZO (Otwinowski, 1993), and reduced with the CCP4 package (CCP4, 1994) (Table 1).

Phase calculations and initial model

A major heavy atom site for for a mercuric derivative (Hg2) was located using RSPS. The remaining heavy atom positions were determined and correlated to each other by cross-difference Fourier calculations. Heavy atom parameter refinement and phasing was performed with VECREF and MLPHARE. The initial MIRAS phasing (figure of merit 0.66 at 2.06 Å) made use of 10 heavy atom derivatives, 7 of which were chemically distinct (Table 1). The electron density map was improved by solvent flattening, histogram matching, and solvent flipping using DM. A bone map of interpretable quality was obtained using the program O (Jones et al., 1991). A polyalanine model of 80 residues derived from the crystal structure of a flavodoxin *Desulfovibrio vulgaris* (Watt et al., 1991), representing the five central β-strands and three helices, was fitted into the bone map. The quality of the density map was gradually improved by three cycles of rigid-body refinement of the polyalanine model at 3.0 Å using XPLOR (Brünger, 1993) (*R* dropped from 58.1 to 47.9%, free-*R* from 63.5 to 50.1%), followed by SIGMAA phase recombination with the MIRAS phases, density modification, and remodeling. At this stage the polyalanine model was extended to 151 alanine residues. After one cycle of simulated annealing and temperature factor refinement using XPLOR, phase recombination, and density modification, the resulting density map at 2.7 Å (*R* 47.2%, free-*R* 49.9%) was used to assign the side chains. A further three rounds of the same procedure, while extending the resolution to 2.3 Å, dropped the *R*-factor to 27.7% (free-*R* 36.9%). All programs were CCP4 (1994) unless otherwise stated.

Table 1. *X-ray data collection and phasing statistics*

	Resolution	R_{merge} (%)	Completeness (%) (reflections)	Redundance	R_{cullis} centric	Phasing power acentric/centric
Native 1	2.06	8.5	99.2 (11,411)	3.5	—	—
Native 2	1.93	8.2	89.2 (13,289)	3.9	—	—
Emp1[a]	2.30	4.5	97.3	3.5	0.66	2.19/1.56
Hg2[a]	2.70	8.8	98.5	3.0	0.82	1.40/0.92
Hg3	3.00	10.1	98.9	3.1	0.87	0.70/0.54
Au1	2.30	5.1	94.0	3.6	0.96	1.24/1.02
Hg4[a]	3.00	11.5	99.7	3.4	0.82	1.25/0.96
Os3[a]	2.30	5.7	97.3	3.9	0.89	0.80/0.64
Pb3	2.50	6.1	97.0	3.5	0.87	0.85/0.72
Co1	2.40	9.5	99.0	3.4	1.14	0.94/0.58
Yb2	2.40	6.2	95.7	3.4	0.94	0.71/0.60
Pt5	2.60	8.3	98.7	3.3	0.97	0.99/0.64

[a] Anomalous signals were used in phase calculation. Emp1: ethyl mercury phosphate; Hg2,3: mercury acetate; Au1: gold cyanide; Hg4: mersalyl acid; Os3: potassium osmiate; Pb3: lead acetate; Co1: cobalt cesium chloride; Yb2: ytterbium chloride; Pt5: potassium tetrachloroplatinate.

Refinement

The structure was further refined by simulated annealing followed by restrained isotropic temperature factor refinement using XPLOR. After another three rounds of refinement, phase recombination, and density modification and remodeling, the *R*-factor had dropped to 23.7% (free-*R* 29.7%) at 8.0–2.07 Å. The refinement was pursued using the higher resolution Native2 data. FMN was placed in the location where unambiguous difference electron density showed its presence and shape during model rebuilding (Fig. 1). Water molecules were added gradually. A further six cycles of model rebuilding using O and refinement against all the data to 1.93 Å resulted in the final model with *R* of 18.9% (free-*R* 24.3%). The final two cycles of refinements were repeated including the data previously omitted for free-*R*. One solvent molecule with very low *B*-factor displayed hepta-coordination. There was also strong $+3\sigma|F_o| - |F_c|$ difference density at this position. This solvent molecule was replaced with a Ca^{2+} ion, although this did not lead to a drop in the free-*R*. The refinement and geometry statistics are shown in Table 2.

Mutagenesis

Mutagenesis was carried out using a variation of the standard Kunkel method (Kunkel, 1985; McDonagh, 1997). Plasmid pMP, containing the coding sequence for the reductase FMN domain cloned into pET15b (Novagen, Madison, Wisconsin) (Smith et al., 1994; Barsukov et al., 1997) was modified to enable production of single stranded DNA by the insertion of the F1 origin from M13 into the unique *Sph*I site. The plasmid was transformed into *Escherichia coli* RZ1032 and single stranded DNA was produced as described in the Sculptor in vitro mutagenesis kit (Amersham International, Amersham, UK). For mutagenesis, 4 pmol of phosphorylated mutagenic oligonucleotide was annealed to approximately 1 μg of single stranded DNA in 1.4 M MOPS, pH 8.0, 1.4 M NaCl in a total volume of 9 μL. Annealing was carried out at 70 °C for 5 min, 37 °C for 30 min, and finally at 4 °C for 5 min. Primer extension was carried out at 37 °C for 30 min with 2 U of DNA polymerase I Klenow fragment (Boehringer Mannheim, Mannheim, Germany), 500 μM dNTPs, 1 mM $MgCl_2$, and 1 U of DNA ligase (New England Biolabs, Beverly, Massachusetts) in a total volume of 20 μL. The reaction was terminated by heating at 70 °C for 5 min, prior to transformation into *E. coli* JM109. Mutagenesis was confirmed by sequencing. Mutants were expressed from *E. coli* BL21 (DE3) grown in LB and purified as reported previously (Zhao et al., 1996; Barsukov et al., 1997).

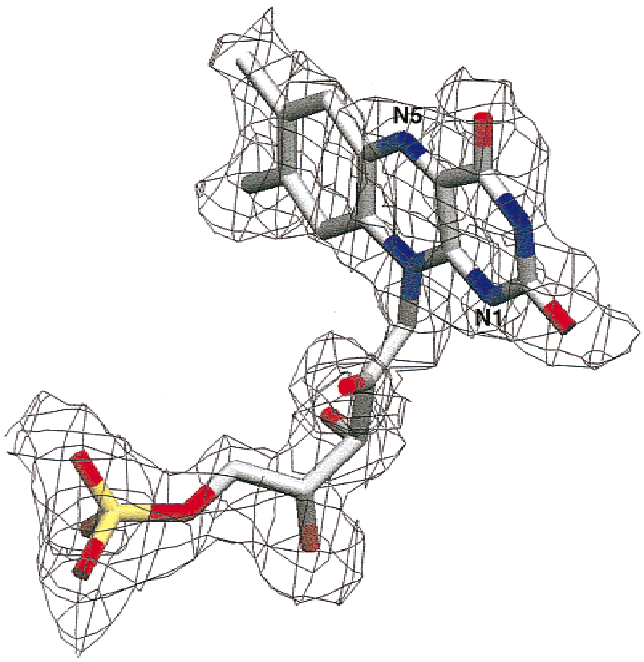

Fig. 1. $|F_o| - |F_c|$ electron density map (contour 1.5σ, 1.93 Å) for the FMN moiety before FMN was fitted, with the final coordinates of FMN superimposed.

Table 2. *Refinement and geometry statistics*

Resolution range (Å)	19.45–1.93
Reflections	13,282
R-factor (%, without σ cutoff)	19.73
Total number of atoms in protein (excluding H)	1,326
Solvent atoms (excluding H)	61
Mean isotropic temperature factor	
Main chain of the protein	17.57
Side chain of the protein	20.99
Cofactor FMN	13.18
Solvent	25.26
Ca^{++} ion	22.37
RMS bond lengths (Å)	0.010
RMS bond angles (°)	1.45
Ramachandran plot	No outliers

Characterization of mutants

Protein concentration was measured using the Bradford method, and FMN was measured spectrophotometrically after releasing it by denaturing the protein by heating to 70 °C. Cytochrome P450-dependent monooxygenase activity was determined using cytochrome P450 2D6 with codeine as substrate as described (Modi et al., 1996). Assay mixtures contained 30 μM P450 2D6, 30 μM P450R-FMN, 30 μM FAD/NADPH domain, 0.01–6 mM codeine and 4 mM NADPH in 0.1 M phosphate buffer, pH 7.5 at 25 °C. Cytochrome *c* reductase activity was measured in 0.1 M phosphate buffer, pH 7.5 at 25 °C with 380 nM FMN domain, 380 nM FAD/NADPH domain, 0.15 mg/mL cytochrome *c*, and 0.2 mM NADPH. The reaction was monitored by the increase in absorbance at 550 nm (ϵ_{550} = 21 mM^{-1} cm^{-1}). Cytochrome *c* was oxidized using potassium ferricyanide immediately before the experiment and used within 1 h.

Coordinates

Coordinates have been deposited in the Protein Data Bank (access no. 1b1c).

Results and discussion

Overall structure

The model of the crystal structure determination (Tables 1 and 2) of the FMN-binding domain of human P450R consists of residues

Glu6 to Val173. The side-chain atoms of Glu82 and Asp100 are not defined by electron density. The seven N-terminal and nine C-terminal residues could not be positioned for lack of density. The high *B*-factors for terminal residues Ser7 and Gly172 point to the high mobility or disorder of both termini, and NMR evidence indicates that at least the 10 C-terminal residues and probably also the N-terminal residues are flexible in solution (Barsukov et al., 1997).

The Ca^{2+} ion is liganded by two oxygen atoms and five water molecules at a distance of ca. 2.4 Å in a distorted bipyramidal arrangement. The two oxygen atoms are provided by the OG atom of Ser104, and the oxygen atom of Thr117 of a symmetry-related molecule. The ion is also connected to the OE1 and OE2 atoms of residue Glu169 from another symmetry-related molecule via hydrogen bonds with three neighboring water molecules. Ca^{2+} is therefore involved in the stabilization of the crystal lattice, in agreement with the critical role of $CaCl_2$ in the crystallization (Zhao et al., 1996).

The overall fold of human P450R-FMN (Fig. 2) is a wound α-β-α fold consisting of five parallel β-strands in the core of the molecule flanked by two helices on one side (α2 and α7) and five on the other. Strand β1 consists of residues 20–25, β2 49–52, β3 72–78, β4 107–114, β5a 138–139, and β5b 144–147. The fifth β-strand is divided into two parts (β5a and β5b) by a four residue stretch of non-β conformation. Helix α1 consists of residues 9 to 15 in the α-helical configuration, α2 30–45 (30–41 α-helix, 42–45 3_{10} helix), α3 54–56 (3_{10} helix), α4 59–67 (3_{10} helix), α5 87–98 (87–89 3_{10} helix, 90–98 α-helix), α6 123–134 (α-helix), and α7 152–171 (α-helix). The locations of these elements of secondary structure are in good agreement (±2 residues) with those identified[5] by NMR in solution (Barsukov et al., 1997), with two minor exceptions: the short 3_{10} helix spanning residues 54–56 was not identified by NMR, due to missing assignments, and, while the existence of a gap in β-strand five around residues 140–144 was clear from the NMR data, its extent could not be accurately defined with the data available.

The cofactor FMN lies on the top of the β-sheet, at the C-terminal ends of the strands (Fig. 2), as seen in the intact rat reductase (Wang et al., 1997). Figure 1 shows the unambiguous electron density map for FMN in P450R-FMN at the end of the refinement before FMN was added into the model.

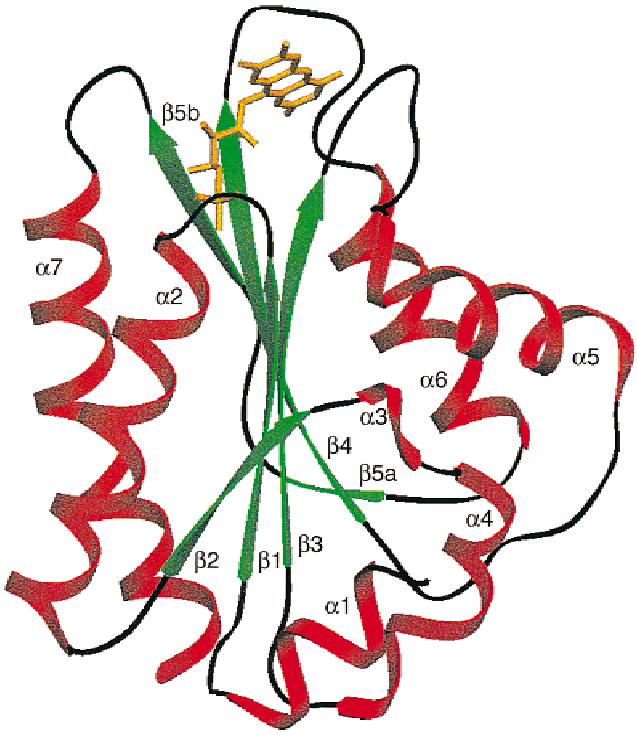

Fig. 2. Ribbon representation (SETOR) of P450R-FMN seen along the plane of the parallel β-sheet with the FMN moiety in brown at the top. The structure consists of a right-handed twisted sheet made up of five parallel β-strands (green) in the core of the molecule flanked by two helices (red) on one side and five on the other. The cofactor FMN lies in a crevice on the top of the β-sheet.

Comparison of the overall structure with flavodoxins and with intact rat P450 reductase

The structure of P450R-FMN was compared with known flavodoxin structures whose sequences are compared with that of P450R in Figure 3. P450R-FMN and all the flavodoxins clearly have a common fold, consisting of a central five-stranded parallel β-sheet flanked on either side by helices. Approximately the same regions of the proteins are involved in FMN binding, and the orientation of the isoalloxazine ring relative to the protein structure is similar in all cases. The conformation of the FMN is also similar; when the isoalloxazine rings are superimposed, the average distance between the phosphorus atom of FMN in P450R-FMN and that in flavodoxins is less than 1.5 Å.

In the flavodoxins, as in P450R-FMN, the fifth β-strand is divided into two (β5a and β5b in P450R-FMN) by a stretch of non-β-strand residues; in the long-chain flavodoxins, there is an insert of about 20 residues at this position. Although the central β-sheet is very similar in all the structures, when the β-sheet of P450R-FMN is superimposed on those of the flavodoxins, the flanking helices on either side are out of register and shifted. As compared to the flavodoxins, P450R-FMN has an extra N-terminal helix, α1, and a short extra 3_{10} helix 3, while helix α4 is longer. The RMS differences in Cα positions between the structure of P450R-FMN and those of the flavodoxins from *D. vulgaris* and *Chondrus crispus* are 1.537 and 1.817 Å, respectively (121 and 114 equivalent Cα atoms). The secondary structure of P450R-FMN is generally in good agreement with that reported by Wang et al. (1997) for the intact rat P450 reductase with the exception of the non-β structure interruption in the fifth β-strand. It is not yet clear whether this difference reflects the higher resolution of the present structure.

The FMN binding site

The resolution of the present structure allows us to describe the binding site for FMN in detail and to compare it to that in the flavodoxins and that reported for the intact rat P450 reductase (Wang et al., 1997). The isoalloxazine ring appears to be planar; its pyrimidine end is slightly buried by two loops, between β3 and α5 (residues 80–83) and β4 and α6 (115–120), while the dimethyl benzene edge is exposed to solvent and forms lattice contacts with

[5] Using the residue numbering and secondary structure designations for P450R-FMN.

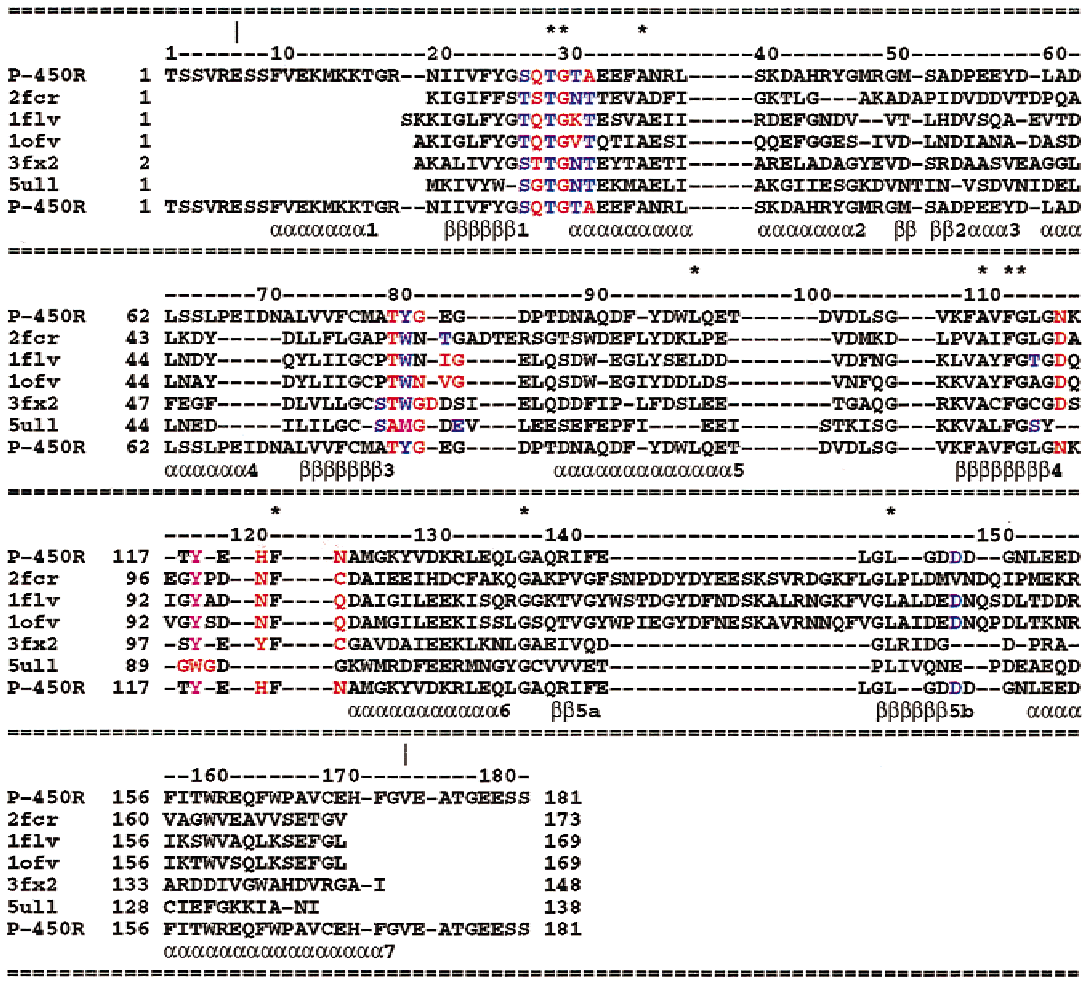

Fig. 3. Sequence alignment based on structural superposition of P450R-FMN with flavodoxins of know structure [*C. crispus* (Fukuyama et al., 1990) (PDB-code 2fcr), *Anabaena* 7120 (Rao et al., 1992) (1flv), *Anacystis nidulans* (Smith et al., 1983) (1ofv), *Clostridium beijerinckii* (Ludwig et al., 1997) (5ull), *D. vulgaris* (Watt et al., 1991) (3fx2)]. The residues that are conserved in P405R-FMN and the flavodoxins are indicated with an asterisk (*). Residues interacting with the cofactor FMN are indicated in blue for side-chain hydrogen bond, red for main-chain hydrogen bond, and purple for hydrophobic interaction.

residues Ser63 and Glu67. The specific interactions between the FMN and the protein are summarized schematically in Figure 4 and compared with those in flavodoxins in Table 3.

The N1, O2, N3, and O4 atoms of the isoalloxazine ring form hydrogen bonds to backbone atoms only of residues Asn115, His120, Asn122 (on the loop between β4 and α6), and Gly81 (on the loop between β3 and α5). The fact that the electronegative atoms of the flavin ring interact only with backbone atoms of the protein appears to be a general feature of the structure of flavodoxins as well as of P450R-FMN (Table 3) and of the intact rat reductase. The nearest atoms to N5, the site of protonation upon reduction, in P450R-FMN are the Cα and amide N of Gly81 (3.6 and 3.8 Å, respectively). No protein atoms or water molecules are within 3.5 Å of N5 in the oxidized state of flavodoxins except in *C. crispus* where the OG of Thr58 is equidistant from O4 and N5 (Table 3). In the intact rat reductase, there is an additional interaction between O4 and the amide N of Gly143 (equivalent to Gly83). Again, it is not clear if this is a difference in interpretation arising from the lower resolution of the structure of the intact rat enzyme or a real difference in structure.

In P450R-FMN, the isoalloxazine ring is sandwiched between the two aromatic side chains of Tyr80 and Tyr118 at nearly the same distance of 3.5 Å; it lies almost parallel to the ring of the outer residue Tyr118, and makes an angle of about 40° with the ring of the inner residue Tyr80. These two tyrosines are in similar positions in the structure of the intact rat enzyme (Wang et al., 1997). Most flavodoxins have a tilted tryptophan for the outer aromatic residue, although in *Clostridium* flavodoxin this is replaced by a methionine.

The pattern of interactions of the ribityl moiety of FMN appears to be conserved among the flavodoxins and P450R-FMN; in all cases, the ribityl O2 interacts with a backbone carbonyl, while ribityl O3 and O4 interact with solvent and/or with side-chain oxygens (or in one case a nitrogen). In the intact rat reductase (Wang et al., 1997), the interaction of the OD2 of the equivalent of Asp148 with the ribityl O4 atom is not present, and there is an additional interaction between the ribityl O2 atom and the carbonyl oxygen of Leu173 (equivalent to Leu113).

The phosphate group of FMN is located at the N-terminal end of helix α2. Three phosphate oxygens make multiple hydrogen bond-

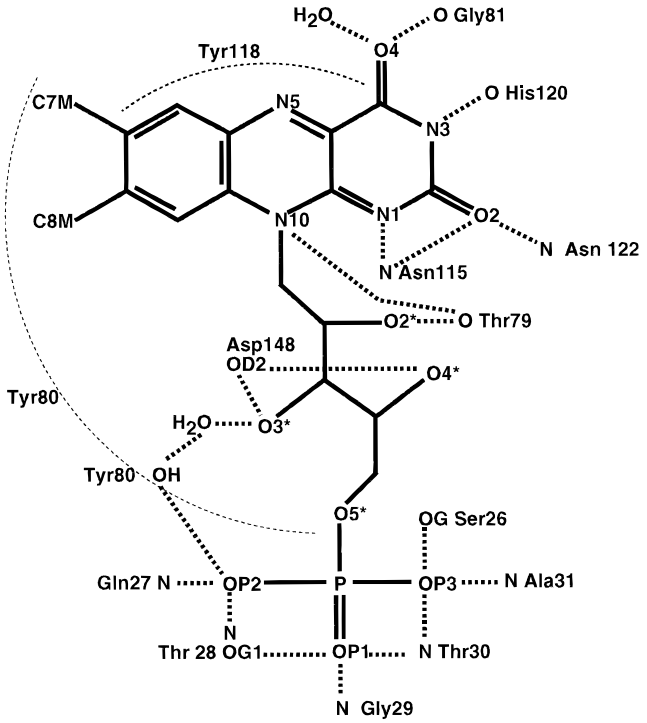

Fig. 4. Schematic diagram of the interactions of the cofactor FMN with the FMN-binding domain of P450R.

ing interactions with backbone NHs of residues 26–31 on the loop between β1 and α2 (Fig. 4; Table 3), and there are hydrogen bonds to the side-chain hydroxyls of Thr28, Ser26, and Tyr80. These extensive hydrogen bonding interactions, together with the electrostatic interaction with the α-helix dipole, stabilize the binding of the FMN phosphate to the protein. Very similar interactions with backbone NHs and side-chain hydroxyls are a general feature of the phosphate binding site of flavodoxins and residues in the loop corresponding to residues 26–31 in P450R-FMN are relatively well conserved in the flavodoxins (Fig. 3). In the 2.6 Å structure of the intact rat reductase (Wang et al., 1997), the hydroxyl group and nitrogen atom of Thr28 appear to make additional interactions with two of the phosphate oxygens that are not seen in P450R-FMN.

It is thus clear that the essential features of the FMN binding site are remarkably conserved between human P450 reductase and the bacterial flavodoxins.

Charge distribution, substrate binding, and electron transfer

Although no direct structural information is yet available for the binding of P450R to its substrates, a number of lines of evidence like have suggested the importance of electrostatic interactions in the binding of P450R to its substrate. For example, neutralization of carboxylate groups on P450R by chemical modification inhibits both cytochrome *c* reductase activity and cytochrome P450-dependent monooxygenase activity (Tamburini & Schenkman, 1986; Nadler & Strobel, 1988), and some of the acidic residues involved have been identified by site-directed mutagenesis of rat liver P450R (Shen & Kasper, 1995). The only known structure for a class II P450 is the haem domain of P450 BM-3 (Ravichandran et al., 1993), in which the proposed reductase binding site is a depression on the proximal side of the haem which has a cluster of positively charged residues, and homology modeling and mutagenesis indicate that this cluster is conserved in eukaryotic class II P450s (Bridges et al., 1998; Peterson & Graham, 1998). Mutagenesis and chemical modification studies of mammalian P450s have also provided evidence for the importance of Lys and Arg residues in reductase binding (e.g., Shimizu et al., 1991).

The FMN-binding domain of P450R has 19 positive and 34 negative charges in 167 residues, giving rise to a negative monopole of −15. The structure shows that the domain is strongly electrically dipolar (677 Debye) with the positive and negative poles located toward the two terminal helices and the area of the FMN binding site, respectively (Fig. 5). The dipole lies roughly in the plane of the central sheet, centered near the center of gravity of the protein, and points from the flavin ring toward the C-terminal ends of helices 1 and 2. The marked separation of charges on the surface of P450R-FMN is very striking, and is likely to be important in binding its electron transfer partners and perhaps also in the electron transfer process itself.

In P450R-FMN, there is a cluster of nine positive charges (residues 12, 14, 15, 18, 37, 40, 43, 44, 48) at a distance of 20–40 Å from the FMN, arising mainly from residues on helix 1 and the C-terminal part of helix 2. This part of the molecule is much more positively charged in P450R-FMN than in flavodoxins, not only because helix 1 is absent in flavodoxins but because the positive residues in the C-terminal half of α2 are poorly conserved in the other proteins in Figure 3. As a result, the molecular dipole is much greater in P450R-FMN than in flavodoxins.

Negative potential is dominant around the FMN binding site, due largely to a cluster of negatively charged residues close to the N1 atom of FMN. This includes Glu82, Asp84, Asp87, Glu119, Asp147, Asp148, Asp149, Asp155 within 15 Å, and Glu32, Glu33, Asp53, Glu55, Asp94, Asp129, Glu142, Glu153, and Glu154 at 15–20 Å. A quarter of all the acidic residues are thus close to the FMN. Although the flavodoxins also have the FMN site surrounded with negative residues, the specific residues are not well conserved.

Of the three loops around the FMN binding site (Fig. 2), the β4-α6 loop (residues 115–122), which contains Tyr118, has a mixed charge distribution, but the other two loops (β3-α5 and β5b-α7) contain three clear clusters of acidic residues, which could form ion-pair interactions with the electron transfer partners. The β5b-α7 loop contains cluster 1, Asp147, Asp148, and Asp149 (of which Asp148 interacts with the ribityl moiety of FMN), and this is closely followed by cluster 2, Glu153, Glu154, and Asp155, at the beginning of helix α7. These two patches correspond to the region of P450R, which was cross-linked to a lysine residue in cytochrome *c* (Nisimoto, 1986) and which has been investigated by site-directed mutagenesis of the rat liver enzyme by Shen and Kasper (1995). On the opposite side of the FMN binding pocket, the β3-α5 loop, which contains the "inner" Tyr80, also contains a third cluster of acidic residues, Glu82, Asp84, and Asp87, which has not previously been investigated.

We have constructed mutants of several residues in these three clusters in human P450R-FMN to investigate their role in the binding of and electron transfer to cytochrome *c* and cytochrome P450 2D6. Their properties are presented in Table 4; although all these substitutions are close to the FMN binding site, and Asp148 interacts with it directly, none of them affected the FMN content of the domain.

Table 3. *Comparison of hydrogen bonding pattern to FMN between P450R-FMN and selected flavodoxins indicated by PDB code (see Fig. 3 for key)*[a]

FMN atom[a]		P450R-FMN	3fx2	2fcr	1flv	5ull	1ofv
N1	3.2 Å	N (N115)	N (D95)	N (D94)	N(D90)	N (D90)	N (G89)
O2	3.0 Å	N (N115)	N (D95)	N (D94)	N(D90)	N (D90)	N(G89)
	2.9 Å	N (N122)	N (C102)	N (C103)	N(Q99)	N (Q99)	N (W90)
					Wat249		N (G91)
							Wat 246
N3	2.9 Å	O (H120)	O(Y100)	O (N101)	O(N97)	O (N97)	OE2 (E59)
O4	3.0 Å	O (G81)	N (D62)	OG1 (T58)	N(G60)	N (V59)	N (E59)
	2.9 Å	Wat241	Wat 6			N (G60)	Wat278
N5	3.8 Å	N (G81)	O (G61)	OG1 (T58)	N (I59)	N (N58)	O (G57)
			N (D62)				
N10	3.3 Å	O (T79)	O (T59)	O (T55)	O(T56)	O (T56)	O (A55)
O2*	2.7 Å	O (T79)	O (T59)	O (T55)	O(T56)	O (T56)	N (A55)
							O (A55)
							Wat 380
O3*	2.8 Å	OD2 (D148)	Wat 51	Wat 40	OD2(D146)	OD2 (D146)	Wat 248
	2.9 Å	Wat278			Wat304	Wat 174	
O4*	3.4 Å	OD2 (D148)	ND2 (N14)	Wat 62	OG1(T88)	Wat 181	OD1 (N11)
			Wat 67		Wat202		OG (S87)
							Wat 253
O5*					OG1(T88)		
OP1	2.5 Å	OG1 (T28)	OG1(T12)	OG1 (T10)	OG1(T12)	N (T11)	N (G8)
	3.3 Å	N (G29)	N (T12)	N (G11)	N (T12)	OG1 (T11)	OG (S54)
	2.7 Å	OG1 (T30)	N (G13)	N (N12)	N (G13)	N (G12)	Wat 245
	2.8 Å	N (T30)	N (N14)	ND2 (N12)	N (K14)	N (V13)	
OP2	2.7 Å	N (Q27)	N (T11)	N (S9)	N (Q11)	N (Q10)	N (T9)
	2.8 Å	N (T28)	OG (S58)	N (T10)	N (T12)	NE1 (W57)	OG1 (T9)
	2.7 Å	OH (Y80)	NE1 (W60)	NE1 (W56)	NE1(W57)		N (G10)
							N (N11)
OP3	2.5 Å	OG (S26)	OG (S10)	OG1(T8)	OG1(T10)	OG1 (T9)	OG (S7)
	3.2 Å	N (T30)	N (T15)	N (T13)	N (T15)	N (T14)	N (T12)
	2.7 Å	N (A31)	OG1(T15)	OG1(T13)	OG1(T15)	OG1 (T14)	OG1 (T12)

[a] Atoms in the ribityl phosphate segment of FMN are indicated with an asterisk.

Of the changes made to acidic residues in the β5b-α7 loop (cluster 1), only the D148N mutation has any effect; it decreases the P450 activity by 70%, while having no effect on the cytochrome *c* reductase activity. Recently Jenkins et al. (1997) have shown that substitutions in the corresponding acidic cluster of *Anabaena* flavodoxin affect its ability to transfer electrons to P450 c17 but not to cytochrome *c*. Contrasting effects are seen for substitution in the acidic patch at the beginning of helix 7 (cluster 2); the E153Q and, to a lesser extent, the E154Q mutations decrease the cytochrome *c* reductase activity (by up to 70%) without affecting the P450 activity. The results for these two clusters are in quantitative agreement with those of Shen and Kasper (1995) on intact rat P450R, notwithstanding the very different assay system used, indicating that different P450s bind in a very similar fashion to the FMN-binding domain of P450R. Finally, substitution of Asp84 or Asp87 in the β3-α5 loop leads to a 25–30% decrease in the P450 activity, without affecting cytochrome *c* reductase activity (Table 4). Each of the individual amino acid substitutions has a relatively modest effect on activity, as might be expected for such a negatively charged region of the protein surface, where removal of a single charge can have only a limited effect on the overall electrostatic interaction. Nonetheless, there is, in excellent agreement with the results of Shen and Kasper (1995), a very clear discrimination between the residues of P450R-FMN, which affect its interaction with cytochrome *c* and those which affect its interaction with cytochromes P450.

Wang et al. (1997) have docked cytochrome *c* into their crystal structure of rat P450R and proposed a model for the structure of the complex. In this model, the region of the surface of the FMN-binding domain, which interacts with cytochrome *c*, consists[6] of the loops β4-α6 (residues 115–122) and β5-α7 (residues 147–151), including cluster 1, Asp147–Asp149. The results of Shen and Kasper (1995), confirmed in the present work, show that the binding of cytochrome *c* is not affected by mutations of residues 147 and 148 in cluster 1, while it is affected by mutation of residues 153 and 154 in cluster 2, which do not form part of the proposed

[6] Using the residue numbering and secondary structure designations for P450R-FMN.

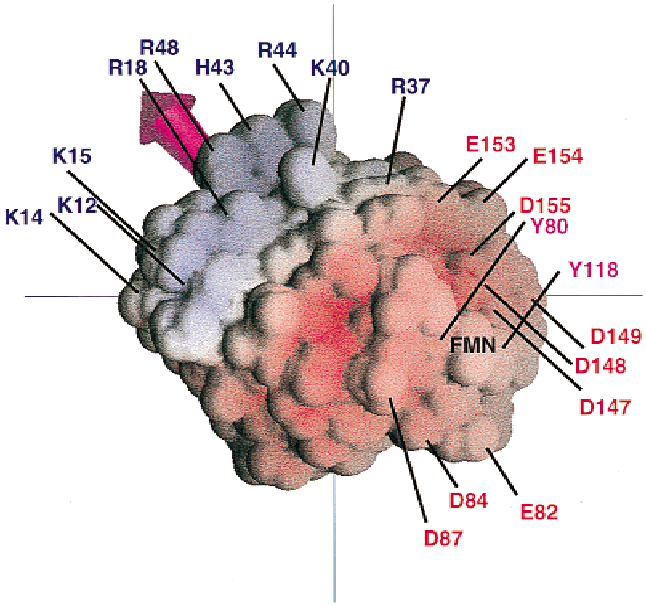

Fig. 5. GRASP electrostatic potential surface of P450R-FMN seen approximately along the plane of the central β-sheet, perpendicular to the strands, from β2 toward β5. The protein shows distinct regions of positive and negative charge giving rise to a dipole roughly in the plane of the sheet parallel to the strands centred near the centre of gravity pointing from the flaving ring toward helix 2. Selected positively and negatively charged residues are indicated in blue and red, respectively.

binding surface. Furthermore, these two residues have virtually no solvent accessibility in the intact rat P450R structure. These results suggest that the position and/or orientation of cytochrome *c* in its complex with P450 reductase is likely to be somewhat different from that proposed by Wang et al. (1997).

The finding that mutation of residues on either side of the FMN binding site, both in cluster 1 and to a lesser extent in the newly identified cluster 3, affect P450 activity suggests that cytochromes P450 bind at the tip of P450R-FMN in such a way as to cover the FMN cofactor. While there may be a substantial overlap between the binding surfaces for cytochrome *c* and cytochrome P450, the mutagenesis results clearly show that there must be differences between them. From the information available, it seems unlikely that the much larger cytochrome P450 molecule could fit into the crystal structure of P450R in the way proposed for cytochrome *c* by Wang et al. (1997). In the crystal structure of the intact reductase, the dimethyl benzene edge of the isoalloxazine ring of FMN, which is exposed in the isolated FMN domain, is covered by the FAD, the two flavins being only 4 Å apart. In this conformation of the intact reductase, it does not appear to be possible for cytochrome P450 to contact the FMN domain in the way described above. This is difficult to reconcile with the mutagenesis results of Shen and Kasper (1995) and those reported here, which are in excellent agreement in identifying the residues important for interaction with P450. The most likely explanation would appear to be that binding of cytochrome P450 over the tip of the FMN domain of P450R requires a movement of the FMN domain relative to the rest of the reductase, which would be facilitated by the flexible linker between the FMN domain and the rest of the molecule. This domain reorganization to allow electron transfer would be analogous to the movement of an iron–sulfur protein domain in cytochrome bc_1 recently described by Zhang et al. (1998). Further structural and spectroscopic studies will be required to seek direct evidence for this in P450 reductase.

Table 4. *Effect of mutation of acidic residues in the FMN domain on the cytochrome c reductase activity and cytochrome P450-dependent monooxygenase activity*

Protein	FMN content (mol/mol)	Cytochrome *c* reductase activity (min^{-1})	P450 2D6 dependent codeine O-demethylation	
			K_M (μM)	k_{cat} (min^{-1})
WT	1.00	31.8 ± 0.8	29 ± 6	0.25 ± 0.01
E82S	0.92	29.1 ± 1.0	22 ± 3	0.26 ± 0.01
D84G	0.94	31.3 ± 2.5	23 ± 2	0.19 ± 0.01
D87S	0.98	32.5 ± 3.0	22 ± 3	0.17 ± 0.01
D147N	0.98	30.7 ± 0.6	21 ± 6	0.22 ± 0.01
D147G	0.94	30.0 ± 1.2	23 ± 2	0.23 ± 0.01
D148N	0.97	34.4 ± 0.7	34 ± 6	0.077 ± 0.003
E153Q	0.98	8.8 ± 1.2	21 ± 2	0.24 ± 0.01
E154Q	0.99	20.3 ± 1.6	25 ± 2	0.26 ± 0.01
D155N	1.05	33.8 ± 1.3	28 ± 6	0.28 ± 0.01

References

Barsukov I, Modi S, Lian LY, Kong Hung Sze KH, Paine MJI, Wolf CR, Roberts GCK. 1997. ^{1}H, ^{15}N, and ^{13}C NMR resonance assignment, secondary structure and global fold of the FMN-binding domain of human cytochrome P450 reductase. *J Biomol NMR 10*:63–75.

Bridges A, Gruenke L, Chang YT, Vakser IA, Loew G, Waskell L. 1998. Identification of the binding site on cytochrome P450 2B4 for cytochrome b_5 and cytochrome P450 reductase. *J Biol Chem 273*:17036–17049.

Brünger AT. 1993. *X-PLOR, version 3.1, A system for X-ray crystallography and NMR*. New Haven, CT: Yale University Press.

CCP4, The Collaborative Computational Project, No. 4. 1994. The CCP4 suite: Programs for protein crystallography. *Acta Crystallogr D50*:760–763.

Enoch HG, Strittmatter P. 1979. Cytochrome b_5 reduction by NADPH-cytochrome P450 reductase. *J Biol Chem 254*:8976–8981.

Fukuyama K, Wakabayashi S, Matsubara H, Rogers LJ. 1990. Tertiary structure of oxidized flavodoxin from an eukaryotic red alga *Chondrus crispus* at 2.35-Å resolution. *J Biol Chem 265*:15804–15812.

Ilan Z, Ilan R, Cinti DL. 1981. Evidence for a new physiological role of hepatic NADPH: Ferricytochrome (P450) oxidoreductase. *J Biol Chem 256*:10066–10072.

Iyanagi T, Mason HS. 1973. Some properties of hepatic reduced nicotinamide adenine dinucleotide phosphate-cytochrome *c* reductase. *Biochemistry 12*:2291–2308.

Jenkins CM, Genzor CG, Fillat MF, Waterman MR, Gómez-Moreno C. 1997. Negatively charged *Anabaena* flavodoxin residues (Asp^{144} and Glu^{145}) are important for reconstitution of cytochrome P450 17α-hydroxylase activity. *J Biol Chem 272*:22509–22513.

Jones TA, Zou JY, Cowan SW, Kjeldgaard M. 1991. Improved methods for building protein models in electron density maps and the location of errors in these models. *Acta Crystallogr A47*:110–119.

Karplus PA, Daniels MJ, Herriot JR. 1991. Atomic structure of ferredoxin-NADP reductase: Prototype for a structurally novel flavoenzyme family. *Science 251*:60–66.

Kunkel TA. 1985. Rapid and efficient site-specific mutagenesis without phenotypic selection. *Proc Nat Acad Sci USA 82*:488–492.

Lu AYH, Junk KW, Coon MJ. 1969. Resolution of the cytochrome P-450 containing ω-hydroxylation system of liver microsomes into three components. *J Biol Chem 244*:23714–3721.

Ludwig ML, Pattridge KA, Metzger AL, Dixon MM, Even M, Feng Y, Swenson RP. 1997. Control of oxidation-reduction potentials in flavodoxin from *Clostridium beijerinckii*: The role of conformational changes. *Biochemistry 36*:1259–1280.

McDonagh PD. 1997. Protein engineering to probe the catalytic mechanism of alpha-class glutathione S-transferases [PhD Thesis]. Leicester, UK: University of Leicester.

Modi S, Gilham DE, Sutcliffe MJ, Lian LY, Primrose WU, Wolf CR, Roberts GC. 1997. 1-Methyl-4-phenyl-1,2,3,6-tetrahydropyrine as a substrate of cytochrome P450 2D6: Allosteric effects of NADPH-cytochrome P450 reductase. *Biochemistry 36*:4461–4470.

Modi S, Paine MJ, Sutcliffe MJ, Lian LY, Primrose WU, Wolf CR, Roberts GC. 1996. A model for human cytochrome P450 2D6 based on homology modeling and NMR studies of substrate binding. *Biochemistry 35*:4540–4550.

Nadler SG, Strobel HW. 1988. Role of electrostatic interactions in the reaction of NADPH-cytochrome *p*-450 reductase with cytochromes *P*-450. *Arch Biochem Biophys 261*:418–429.

Nisimoto Y. 1986. Localization of cytochrome *c*-binding domain on NADPH-cytochrome P-450 reductase. *J Biol Chem 261*:14232–14239.

Ortiz de Montellano PR. 1995. *Cytochrome P450: Structure, mechanism and biochemistry*, 2nd ed. New York, NY: Plenum Press.

Otwinowski Z. 1993. Oscillation data reduction program. In: Sawyer L, Isaacs N, Bailey S, eds. *Proceedings of the CCP4 study weekend: Data collection and processing*. Daresbury: SERC, Daresbury Laboratory. pp 56–62.

Peterson JA, Graham SE. 1998. A close family resemblance: The importance of structure in understanding cytochromes P450. *Structure 6*:1079–1085.

Philips AH, Langdon RG. 1962. Hepatic triphosphopyridine nucleotide-*cytochrome c* reductase: Isolation, characterization, and kinetic studies. *J Biol Chem 237*: 2652–2660.

Porter TD. 1991. An unusual yet strongly conserved flavoprotein reductase in bacteria and mammals. *TIBS 16*:154–158.

Porter TD, Kasper CB. 1986. NADPH-cytochrome P450 oxidoreductase: Flavin mononucleotide and flavin adenine dinucleotide domains evolved from different flavoproteins. *Biochemistry 25*:1682–1687.

Rao ST, Shaffie F, Yu C, Satyshur KA, Stockman BJ, Markley JL, Sundaralingam M. 1992. Structure of the oxidized long-chain flavodoxin from *Anabaena* 7120 at 2 A resolution. *Protein Sci 1*:1413–1427.

Ravichandran KG, Boddupalli SS, Hasemann CA, Peterson JA, Deisenhofer J. 1993. Crystal structure of hemoprotein domain of P450BM-3, a prototype for microsomal P450s. *Science 261*:731–736.

Schacter BA, Nelson EB, Marver HS, Masters BSS. 1972. Immunochemical evidence for an association of heme oxygenase with the microsomal electron transport system. *J Biol Chem 247*:3601–3607.

Shen AL, Kasper CB. 1995. Role of acidic residues in the interaction of NADPH-cytochrome P450 oxidoreductase with cytochrome P450 and cytochrome *c*. *J Biol Chem 270*:27475–27480.

Shimizu T, Tateishi T, Hatano M, Fujii-Kuriyama Y. 1991. Probing the role of lysines and arginines in the catalytic function of cytochrome $P450_d$ by site-directed mutagenesis. *J Biol Chem 266*:3372–3375.

Smith GCM, Tew DG, Wolf CR. 1994. Dissection of NADPH-cytochrome P450 oxidoreductase into distinct functional domains. *Proc Natl Acad Sci USA 91*:8710–8714.

Smith WW, Patteridge KA, Ludwig ML. 1983. Structure of oxidized flavodoxin from *Anacystis nidulans*. *J Mol Biol 165*:737–755.

Tamburini PP, Schenkman JB. 1986. Differences in the mechanism of functional interaction between NADPH-cytochrome P-450 reductase and its redox partners. *Mol Pharmacol 30*:178–185.

Wang M, Roberts DL, Paschke R, Shea TM, Masters BSS, Kim JJP. 1997. Three-dimensional structure of NADPH-cytochrome P450 reductase: Prototype for FMN- and FAD-containing enzymes. *Proc Nat Acad Sci USA 94*:8411–8416.

Watt W, Tulinsky A, Swenson RP, Watenpaugh KD. 1991. Comparison of the crystal structures of a flavodoxin in its three oxidation states at cryogenic temperatures. *J Mol Biol 218*:195–208.

Williams CH Jr, Kamin H. 1962. Microsomal triphosphopyridine nucleotide-cytochrome *c* reductase of liver. *J Biol Chem 237*:587–595.

Zhang ZL, Huang LS, Shulmeister VM, Chi YI, Kim KK, Hung LW, Crofts AR, Berry EA, Kim SH. 1998. Electron transfer by domain movement in cytochrome bc_1. *Nature 392*:667–684.

Zhao Q, Smith G, Modi S, Paine M, Wolf RC, Tew D, Lian L-Y, Primrose WU, Roberts GCK, Driessen HPC. 1996. Crystallization and preliminary X-ray diffraction studies of human cytochrome P450 reductase. *J Struct Biol 116*:320–325.